

Spring 4-26-2022

The Synthesis and Purification Methodology of an Intermolecular Pyrophosphate Sensor: Applications for the Quantitative Polymerase Chain Reaction

Ethan Gevedon
ethandg@bgsu.edu

Follow this and additional works at: <https://scholarworks.bgsu.edu/honorsprojects>

 Part of the [Analytical Chemistry Commons](#), [Biotechnology Commons](#), [Genetics Commons](#), [Organic Chemistry Commons](#), and the [Other Genetics and Genomics Commons](#)

[How does access to this work benefit you? Let us know!](#)

Repository Citation

Gevedon, Ethan, "The Synthesis and Purification Methodology of an Intermolecular Pyrophosphate Sensor: Applications for the Quantitative Polymerase Chain Reaction" (2022). *Honors Projects*. 688.
<https://scholarworks.bgsu.edu/honorsprojects/688>

This work is brought to you for free and open access by the Honors College at ScholarWorks@BGSU. It has been accepted for inclusion in Honors Projects by an authorized administrator of ScholarWorks@BGSU.

**The Synthesis and Purification Methodology of an Intermolecular Pyrophosphate
Sensor: Applications for the Quantitative Polymerase Chain Reaction**

By: Ethan D. Gevedon

Advisors:

Dr. Pavel Anzenbacher Jr.

Dr. Julia Halo

Introduction:

Phosphate anions are a ubiquitous species in many sectors of industry, agriculture, and the biological sciences. One such species is the Pyrophosphate (PPi) anion. It is prevalent within many biological processes, is linked to many diseases, and is involved with the mechanism of several biotechnological applications. ¹⁻⁴ Phosphate anions share similar electronic and molecular structure to which makes the selective sensing of such species difficult. The prevalence of PPi necessitates the development of molecular sensors capable of selective detection and quantification of PPi over other commonly present phosphate species such as hydrogen phosphate (HPO_4^{2-}), nucleotide triphosphates (NTPs), nucleotide diphosphates (NDPs), nucleotide monophosphates (NMPs), etc. Selective detection of PPi over other common biological phosphates would allow for the circumvention of several drawbacks to biotechnological applications such as with pyrosequencing and quantitative polymerase chain reaction. ^{1,5,6}

Several sensor systems for the selective detection of PPi have been reported: To date, several systems have employed zinc 2+ (Zn^{2+}) ion coordinated to dipicolylamine (dpa) as the active site for PPi coordination. Modification of the molecular frameworks and has allowed for the synthesis of selective and sensitive molecular sensors capable of PPi detection over other anionic analytes in aqueous media. ⁷⁻¹¹ One system reported in 2008 by the team of Nonaka et al, utilized a N-Zn-DPA, N'-meta phenylboronic acid functionalized ethylene diamine (Figure 1) and alizarin red S (ARS) fluorescent reporter for the selective detection of PPi. ¹⁰ While this system proved to be effective at selective, turn-on, fluorescence quantification of PPi, the synthesis and purification of the sensor scaffold was unsatisfactory and the applicability of this sensor system in real-world, biotechnological applications was not determined. ¹⁰

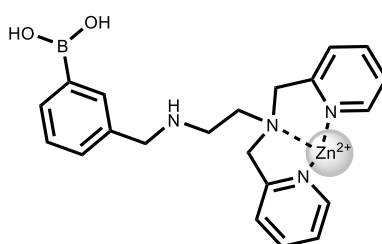


Figure 1: Reported molecular scaffold capable of selective PPi coordination.

The polymerase chain reaction (PCR) allows for the selective amplification of a target DNA sequence from a minute genomic DNA sample into several million copies of a single target DNA sequence. ^{12,13} The process of PCR is fairly straight forward: to begin, the DNA double helix is denatured into single stranded (ssDNA) upon heating. Cooling the sample slightly allows for DNA specific primers to anneal to the gene target to be replicated. The sample is the heated and thermostable DNA polymerase begins

replicating the gene fragment from the free 3'-OH functional groups provided by the DNA primers. This process is replicated for multiple cycles until it is determined that the gene sequence has been amplified to an extent great enough for further genomic analysis. ⁽¹²⁻¹⁴⁾

Advancements in PCR technology have allowed for quantitative measurements of DNA replication to be performed (qPCR). ^{5,6} Real time detection of DNA replicons is monitored by fluorescent measurements of the DNA molecules for which two major classes dominate. The first class are sequence non-specific, DNA intercalator dyes such as SYBR Green; increased fluorescence as a function of increased DNA intercalation permits quantification. ^{2,14,15} The second method, uses fluorescently labeled oligonucleotide primers (i.e. TaqMan probes) that produce a fluorescence response upon incorporation into the DNA sequence. ^{15,16} While both methods are widely available, these methods suffer from several drawbacks. Intercalator dyes suffer from low selectivity to any DNA sequence and result in subsequent false positives. Similarly, the TaqMan hybridization probes are quite costly and must be designed for the specific gene sequence of interest. To the best of our knowledge, no fluorescent sensor within qPCR has been developed that uses the PPI molecule as the analyte of interest. The improved PPI sensor system has the potential to provide a solution to the downsides of the two common quantification techniques and serve as a bridge between both options currently used for real time DNA quantification.

Within this report, we propose the improved synthesis and purification of this sensor scaffold on the gram scale. Likewise, the use of our prepared fluorescent dye, **mCPF** is used as an alternative fluorescent reporter to which will be used in the molecular sensor system (Figure 2). Finally, the sensor system will be applied to the qPCR reaction to determine its applicability as an alternative fluorescent reporter for effective DNA replication quantification.

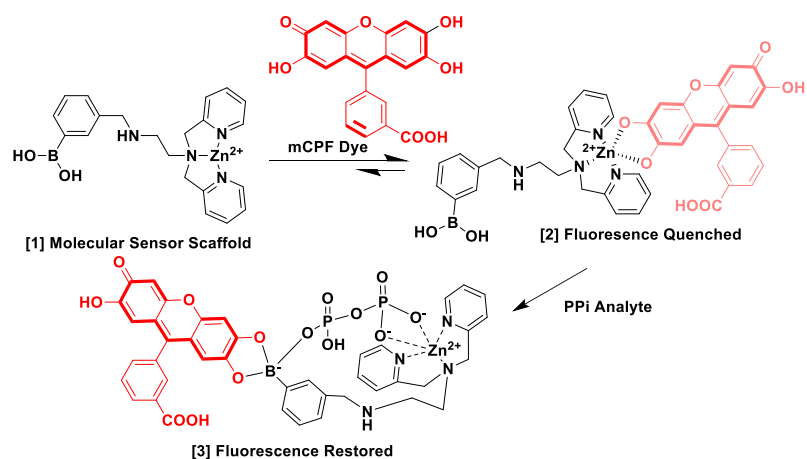


Figure 2: Proposed mechanism of PPI quantification by the sensor system using mCPF.

Results and Discussion:

Synthesis and Optimization:

The gram scale synthesis of the dipicolylamine functionalized ethylenediamine (DPA-en) was performed and used for preparation of the PPI sensor scaffold (N-3-Dihydroxyborylbenzyl-N',N'-bis(2-pyridylmethyl)ethylenediamine molecular scaffold). DPA-en precursor synthesis is described within the experimental section below.

The synthesis of sensor scaffold (1) was previously performed using a two-pot reductive amination with sodium borohydride under our optimized reaction conditions (Figure 3). Through several screening reactions, it was determined that dichloroethane (DCE) was the optimal solvent (61.4% relative yield) followed closely by both ethanol (EtOH) (58.4% relative yield) and MeOH (55.4% relative yield). The retention time of the target peak for all runs were consistent at $t_R \sim 22.184$ minutes. The HPLC chromatogram from the reaction using DCE as solvent and MALDI from the reaction in which EtOH was used are provided and show the presence of the target compound (Figures E3 and E4): both reactions resulted in the same t_R and MALDI was analyzed for the sample synthesized in EtOH to determine the nature of the novel product peak. It was also determined that the addition of acetic acid (AcOH) decreased the formation of product under all solvent conditions and severely hindered product formation in the protic solvents: it is hypothesized that the imine intermediate is unstable under acidic conditions and is rapidly degraded before reduction of sodium borohydride can occur. Likewise, the degradation of sodium borohydride before the complete reduction of the intermediate imine is expected to occur.

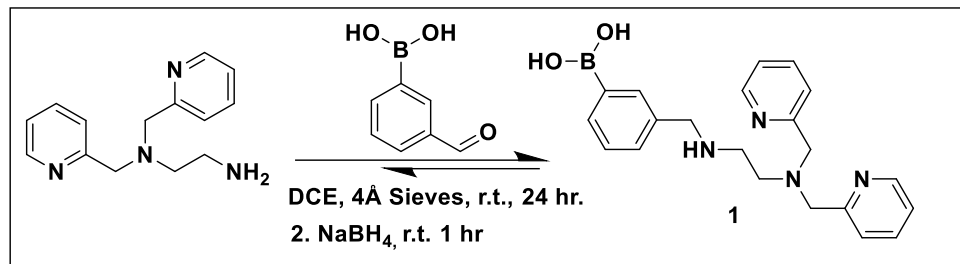


Figure 3: Synthesis of molecular sensor scaffold from DPA-en and 3-formylphenylboronic acid by reductive amination.

From the optimized conditions, the reaction was scaled-up to the 100 mg (DPA-en) scale in DCE: the effectiveness of product purification by automatic column chromatography (ACC) was also determined. Only a portion of the crude product material was soluble in the eluent 95:5 (H₂O:MeOH with 0.1% TFA) used for wet loading on the reverse phase column; a second purification was performed by dissolving the sample into MeOH (Figures 4 and 5 depict the first and second purifications respectively). NMR results from both purifications of the crude product showed high levels of 3-formylphenylboronic acid (3-FPBA) starting material and a lack of product formation (Figure 6). Pelletized NaBH₄ was used for the reduction and is insoluble in DCE. The lowered surface area was expected to be the cause of a lack of product formation.

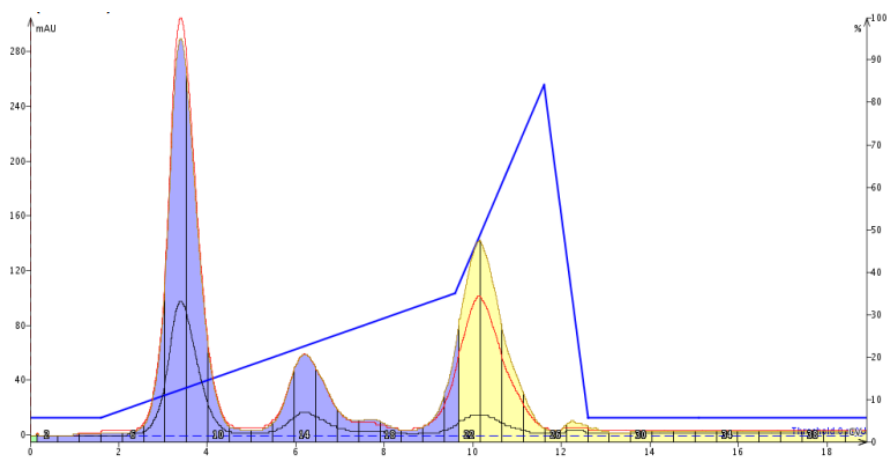


Figure 4: Automatic column chromatogram of eluent soluble crude.

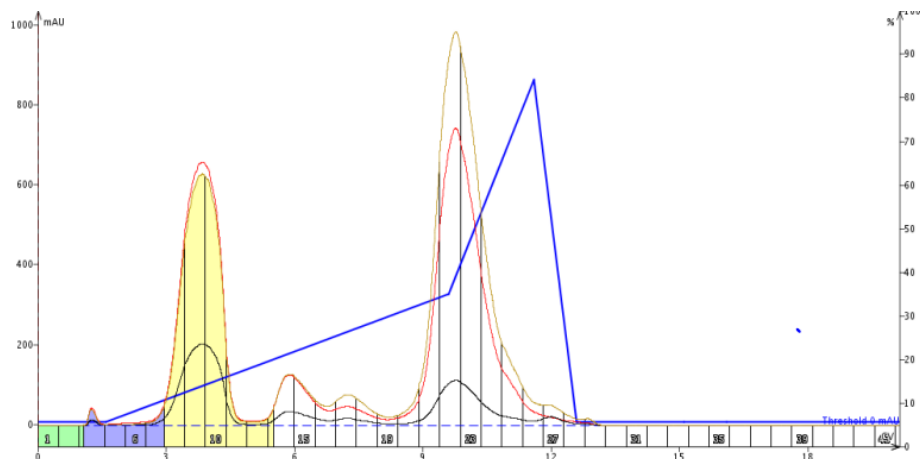


Figure 5: Automatic column chromatogram of MeOH soluble crude.

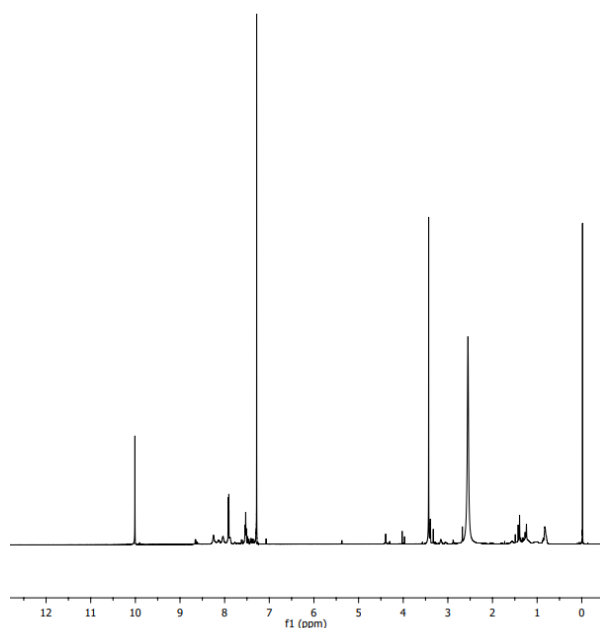


Figure 6: NMR of fractions 19-25 of the eluent soluble crude.

To improve upon the reaction, dry MeOH was used over DCE to improve upon the solubility of the NaBH_4 . Likewise, a 4-molar equivalence excess of NaBH_4 was used to assure complete reduction of the imine. 894.8 mg of crude product obtained and was purified by RP-AC chromatography. However, this overloaded the column (Figure 7): fractions 10-20 were collected and the NMR showed the presence of dirty product (Figure 8). A second purification yielded fractions 17-35 for which the NMR showed to be a cleaner product (Figure 9). However, there were several peaks corresponding to impurities within the NMR spectrum. Figure 8 shows the presence of more than one peak to which explains the impurities within the NMR spectrum. The goal of the scaled-

up reaction was to perform the cheaper and more rapid RP-AC chromatography instead of RP-HPLC purification to generate a fluorescence experiment and qPCR ready molecular scaffold compound. The low resolution of RP-AC made this unachievable and thus further HPLC purification of the pre-purified RP-AC compound was performed.

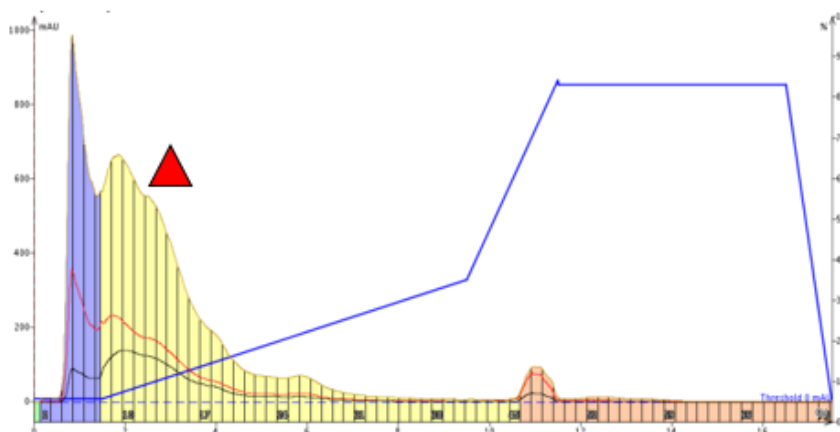


Figure 7: Chromatogram of overloaded column: fractions 10-20 (red triangle) collected for repurification.

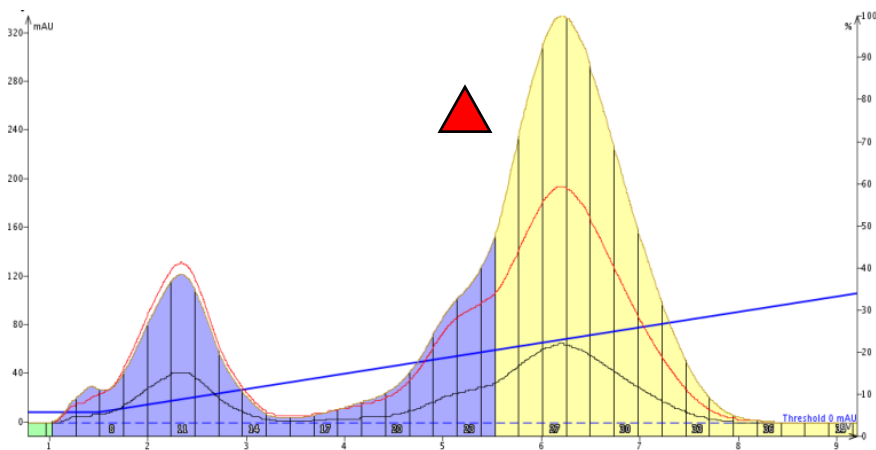


Figure 8: Chromatogram of second purification to yield the pre-purified sensor scaffold: fractions 17-35, red triangle, collected for further purification.

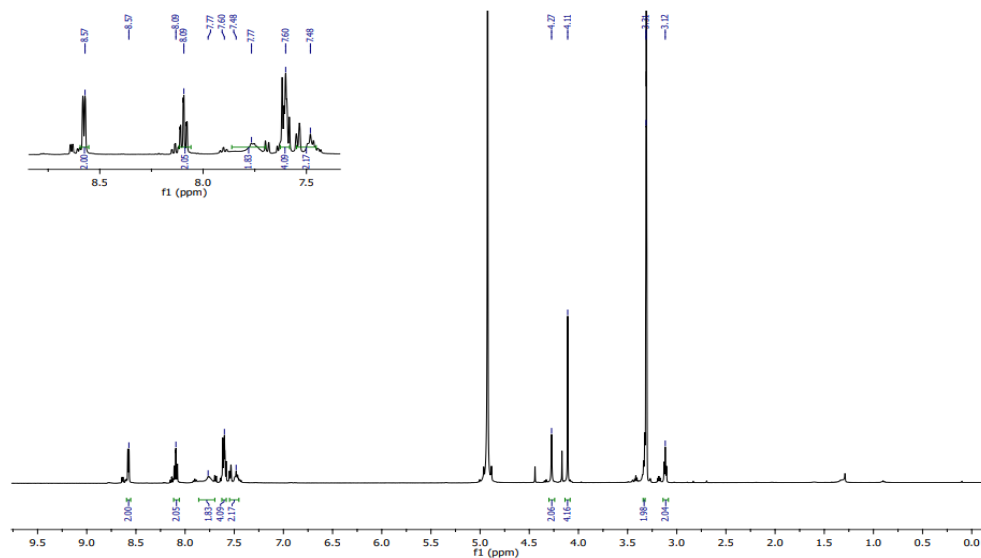


Figure 9: NMR of RP-AC purified sensor scaffold: several impurities are present which elicit the need for further RP-HPLC purification.

HPLC purification of the compound was continued using an optimized condition (95-60% H₂O, 25 minutes). Several purifications were performed on the semi-preparative scale to yield 33.96 mg of purified product. The HPLC chromatogram showed the presence of several impurities surrounding the target compound and confirmed the requirement of HPLC purification to prepare the sensor scaffold (Figure 10). ¹H and ¹³C NMR of the HPLC purified compound were taken to which the hydrogen showed all correct peaks and splitting for the compound while the ¹³C spectrum was missing several peaks due to the low signal to noise ratio of the experiment (Figures 11 and 12). ESI-MS also confirmed the presence of the compound (M+1) m/z = 377.20 (Figure 13). M+14 was also present and is due to the presence of the formation of a methyl boronate ester during ionization under ESI conditions. All analysis concludes that the synthesis and purification of the sensor scaffold was successful.

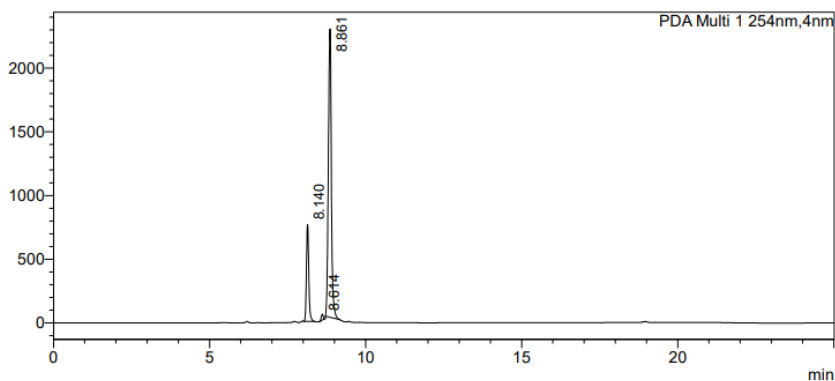


Figure 10: HPLC chromatogram of the purified sensor scaffold compound.

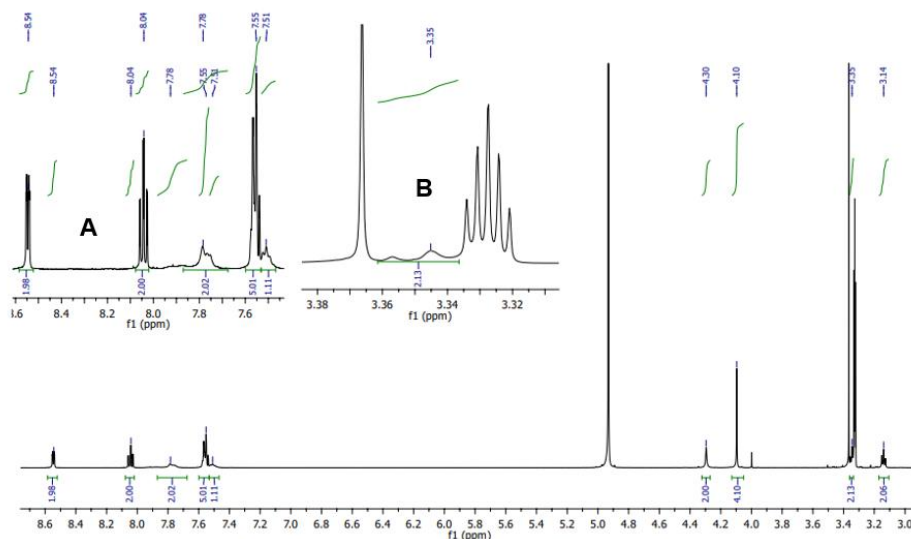


Figure 11: ^1H NMR of the purified sensor scaffold. Expanded regions show the multiplicity of the aromatic region (A) and the obstruction of a triplet by the quintet of MeOD (B)

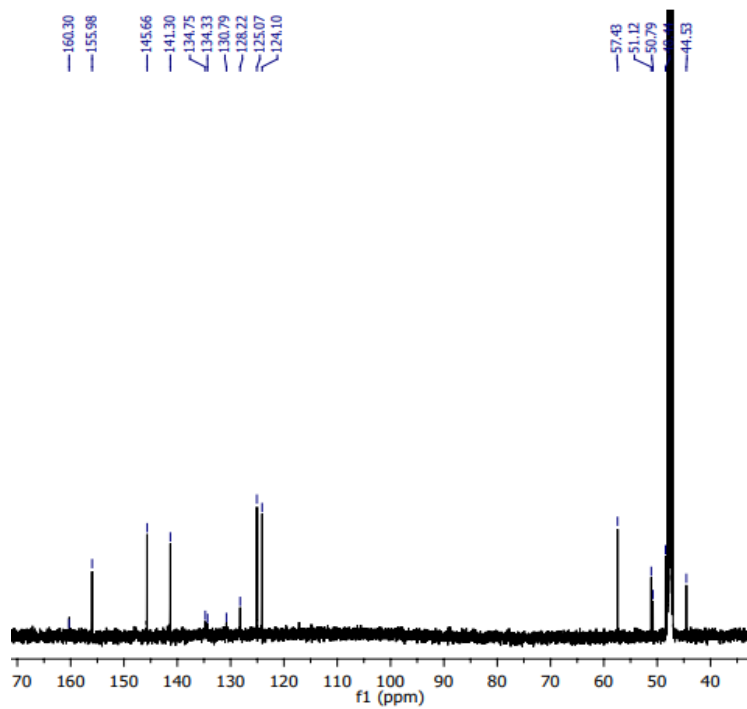


Figure 12: ^{13}C NMR of RP-HPLC purified sensor scaffold.

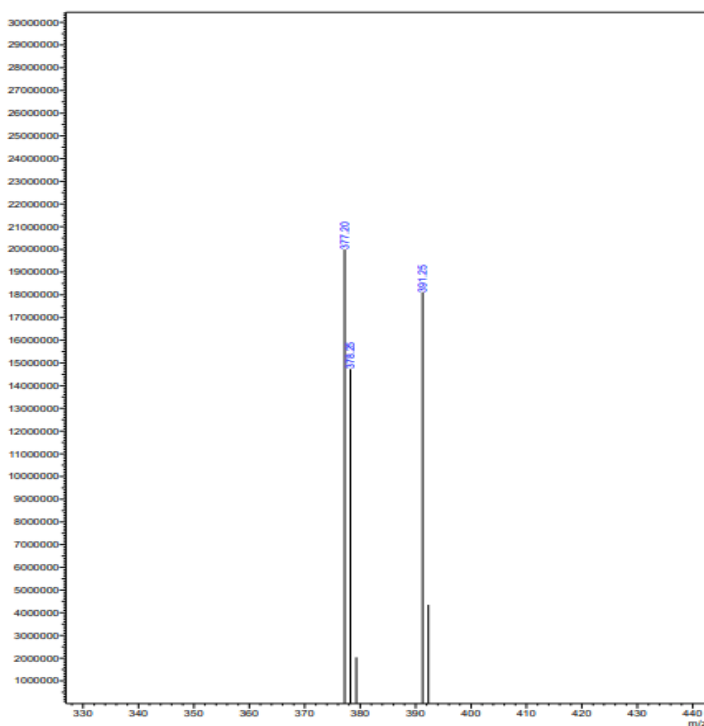


Figure 13: ESI-MS of the purified sensor scaffold: $M+1 = m/z$ 377.20.

The TFA buffered eluent used for HPLC purification has the potential to react with the basic amines on the sensor scaffold compound to form an ammonium salt with the trifluoroacetate counter anion. For further investigation into this compound's fluorescence applications, the free base is required to assure proper concentrations of solutions are prepared from the stock sample. The treatment and extraction of the compound with saturated sodium bicarbonate solution resulted in the evolution of gas and a confirmation that there was an acidic species present within the purified sample. The following DCM extractions yielded 11.0 mg of product. Further NMR and ESI/MS analyses were unable to be performed due to time constraints, but the product is presumed to be the purified basic sensor scaffold.

The final synthetic step in the generation of the active sensor scaffold complex is its complexation to $Zn(NO_3)_2$. Reacting the RP-ACC purified compound with $Zn(NO_3)_2$ in MeOH followed by recrystallization in dry THF yielded a fine yellow crystalline powder. From 1H NMR analysis, it was determined that the compound was impure as the sample appeared to contain a mixture of coordinated and non-coordinated sensor scaffold to $Zn(NO_3)_2$ (Figure 14). However, MALDI analysis showed the presence of characteristic peaks from metal coordination and the fragment patterns of several peaks followed this pattern Figure (15). The MALDI spectrums did not show the presence of the $M+1$ peak for the Zn coordinated compound, and thus it may have undergone complexation or fragmentation during ionization. Absolute determination of the formation of the sensor scaffold could not be determined from MS analysis. With the poor purification

procedures through recrystallization, formation of the active sensor scaffold prior to fluorescence measurements may be difficult and an *in-situ* approach to form the sensor complex may be required. However, as the equilibrium constant between the sensor scaffold and $\text{Zn}(\text{NO}_3)_2$ is not known, a molar excess of $\text{Zn}(\text{NO}_3)_2$ may be required to form the active sensor complex to produce a high signal to noise ratio during sensing: this may be problematic for biological applications where high, excess concentrations of free Zn^{2+} may alter enzyme activity and efficiency (i.e. DNA polymerase in the qPCR reaction).

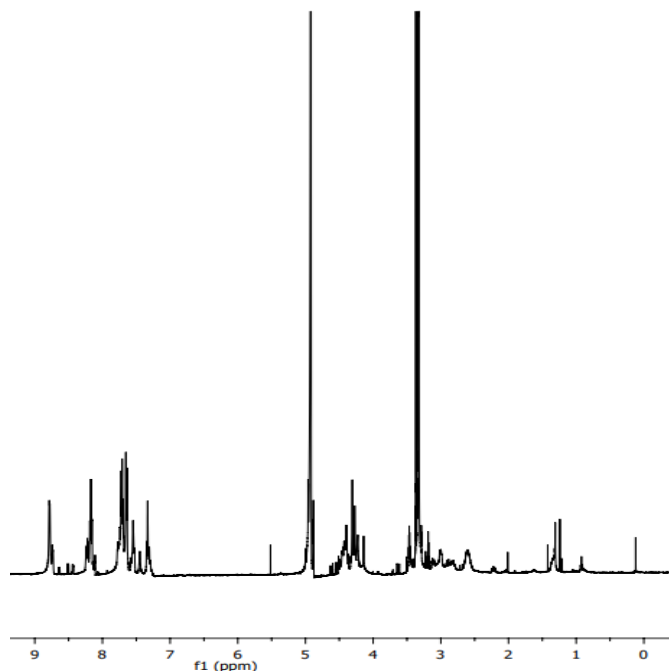


Figure 14: ^1H NMR of $\text{Zn}(\text{NO}_3)_2$ coordination reaction: impurity of the product is depicted.

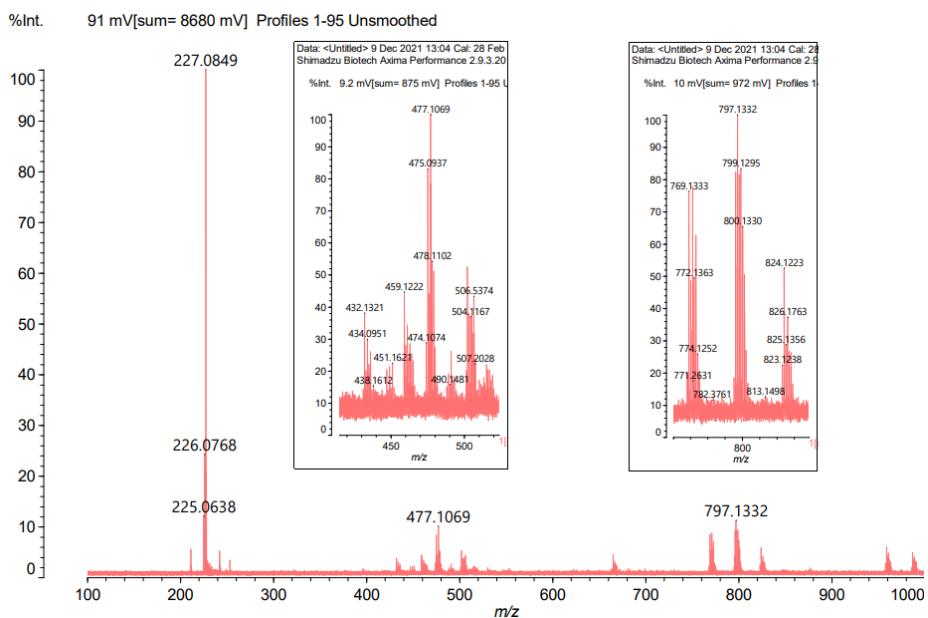


Figure 15: MALDI mass spectrum depicting characteristic metal coordinated peaks but missed the product M+1 peak.

The presence of free Zn^{2+} may interfere with the Mg^{2+} cofactor required for Taq-polymerase to polymerize DNA. To determine the effect of free Zn^{2+} and determine an applicable range of free $Zn(NO_3)_2$ concentration that can be present within the qPCR reaction without inducing detrimental effects, an addition of 0.5 -5 μM Zn was added to a $\Delta\Delta Cq$ qPCR reaction. This method compares the relative expression level of a target gene to a control gene of known expression within the genome. For this experiment, GapDH to Env genes from genomic canine sources were analyzed. This experiment calculates a critical threshold value (C_T), which is the replication cycle where quantization of the replicated DNA becomes statistically significant, for each gene. Mean critical threshold values, C_T values, (triplicate of three with inconclusive results excluded) allows for the comparison of expression levels between the two genes of interest. From this experiment, negligible to indeterminate change in critical threshold values as a result in the change in concentration of $Zn(NO_3)_2$ (Table 1 and Figure 16). From the lack of evidence supporting the decrease in Taq-polymerase efficiency as a result of increasing free Zn concentration, the inclusion of a molar excess of Zn to afford the active sensor scaffold in situ is achievable up to an excess of 5.0 μM $Zn(NO_3)_2$. This wide tolerance will allow for the easy determination of optimal molar equivalencies of sensor scaffold and $Zn(NO_3)_2$ and allow for the optimization of sensor system concentration to DNA concentration to achieve a high signal to noise ratio.

Table 1: Mean C_T values for Env and GapDH gene at varying $Zn(NO_3)_2$ concentrations.

| $[Zn(NO_3)_2]$ μM | Gene Target | C_T Mean |
|---------------------------|----------------|------------|
| 0.0 | Env | 7.640042 |
| 0.5 | Env | 8.129394 |
| 1.0 | Env | 7.892813 |
| 2.0 | Env | 7.408018 |
| 3.0 | Env | 7.893672 |
| 4.0 | Env | 6.713539 |
| 5.0 | Env | 7.693789 |
| 0.0 | GapDH | 8.11347 |
| 0.5 | GapDH | 8.249734 |
| 1.0 | GapDH | 7.732111 |
| 2.0 | GapDH | 7.872323 |
| 3.0 | GapDH | 7.876539 |
| 4.0 | GapDH | 7.09585 |
| 5.0 | GapDH | 7.770018 |

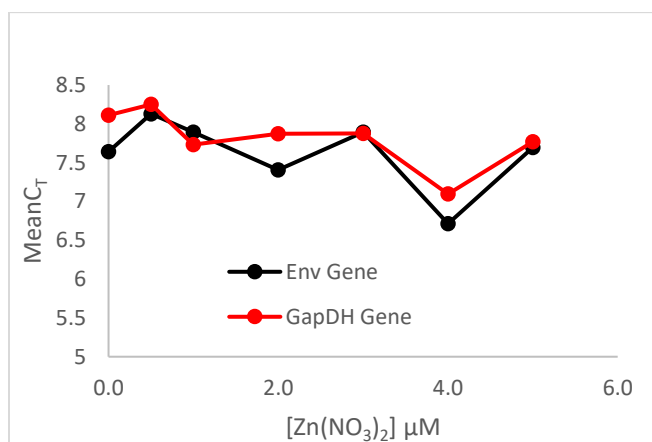


Figure 16: Mean C_T versus $[Zn(NO_3)_2]$ (μM) for the Env and GapDH genes.

Through much research, the development of optimized synthetic conditions and purification methods was finalized for the sensor scaffold compound. While we were hopeful that the sensor compound would be able to be purified solely by RP-ACC techniques, several impurities with similar retention times remained with the product peak. However, both the sensitive nature of fluorescent emission signaling, and the goal of using the sensor system within qPCR, a sensitive biotechnology system, requires the sample to be of the highest purity possible: therefore, RP-HPLC purification was still required to isolate the compound. These extra purification steps may hinder the affordability of such a system as HPLC purification is a more material intensive, and time intensive purification method. If the reaction was scaled-up to the industrial scale,

the use of an industrial, preparatory HPLC system may improve the practicality of the purification techniques both in time and materials consumed.

Beyond the successful scaled-up synthesis and purification of the sensor scaffold, research into the final coordination reaction with $\text{Zn}(\text{NO}_3)_2$ and the application of the sensor system (fluorescence measurements and qPCR fluorescent reporter) had to be halted due to personal time constraints and health issues that were making completion of application research impossible. In accommodation to the remainder of research to be completed, an analysis and discussion of what research is left to be undertaken will follow.

Implications of Future Research, Research Lessons, and Conclusions:

Several key areas of research remain to be investigated to develop the sensor system and to test its application in the qPCR reaction. Due to time constraints, I was unable to complete this avenue of research and a discussion into the remaining steps is provided.

The next phase of research would focus on fluorescence measurements of the mCPF dye and active sensor complex (**ss-PPI-mCPF**). Both species have their own unique, but closely related excitation and emission as a result of modulation of the emission frequency of mCPF when interacting with the sensor scaffold boronic acid.

Both of these species are in equilibrium and the quenched species serves as an equilibrium intermediate (Figure 2): as a result, free mCPF will be present within the solution and will produce a nonzero background fluorescence. To overcome this, and determine the optimal component composition, fluorescence titrations would be performed. Titrations of the sensor scaffold with $\text{Zn}(\text{NO}_3)_2$ would need to be performed to determine the equilibrium constant between the sensor scaffold and $\text{Zn}(\text{NO}_3)_2$: simultaneously, the molar ratio of $\text{Zn}(\text{NO}_3)_2$ required to effectively quench mCPF and the possibility for the requirement of a molar excess of $\text{Zn}(\text{NO}_3)_2$ would be determined. The molar ratio and free Zn^{2+} in solution should be optimized to the conditions determined from the $\text{Zn}(\text{NO}_3)_2$ screening qPCR reactions. The determination of the equilibrium constant and data from the fluorescence experiments would allow for the determination of the background fluorescence caused by mCPF. A second set of titrations would serve to optimize the molar ratio of mCPF dye to sensor scaffold to achieve a high signal to noise ratio within the system: a 1:1 ratio is hypothesized to be optimal to minimize background fluorescence from free mCPF dye.

Titrations of the quenched sensor system with PPI and other phosphate analytes would then be performed. From this analysis, several characteristics of the system would be optimized. First, the fluorescence titration with PPI would allow for the

determination of an optimal emission wavelength to be used in the qPCR instrument: the optimum emission wavelength would be at which the intensity of emission increases with increasing [PPi] μM . The increase in signal would be due to only the shift in equilibrium towards (**ss-PPi-mCPF**) and would result in the increase of the signal to noise ratio for the system.

Fluorescence titrations with other phosphate analytes, especially dNTPs and DNA, would be required to determine the selectivity of the active sensor scaffold to PPi. A low selectivity for PPi would result in a low signal to noise ratio due to background fluorescence from phosphate coordination. Previous results with ARS as the reporter dye found high selectivity for PPi over other biologically active phosphates but this does not preclude the selectivity for the system using mCPF as a reporter dye.¹⁰ Because of this, the equilibrium constant between this sensor system and PPi must be several magnitudes higher than with other phosphates to minimize the background fluorescence from the total non-PPi phosphate concentration which will remain constant as dNTPs are incorporated into the gene sequence. qPCR research would be performed after the optimized ratio of system components was determined, optimal emission wavelength discovered, and confirmation of a high relative equilibrium constant for the sensor system and PPi over other phosphate analytes.

qPCR experiments would require several optimizations of the instrumentation and system component ratios to achieve relevant quantization within qPCR. Most qPCR instruments work under specific dye channels (i.e. SYBR green, etc.) while some have the ability to create and calibrate the system for custom synthesized dyes.¹⁷ The system would be best optimized under such a custom calibration using the excitation and emission wavelengths determined from the fluorescence titrations of (**ss-PPi-mCPF**). However, the similar nature of mCPF and SYBR green dyes would elicit the potential use of the sensing system within the SYBR green fluorescence channel. This would result in a tradeoff system performance: the use of a custom calibration would result in a higher signal to noise, but this may be limited the applicability of the system for all qPCR instruments. Performing the experiment under the SYBR green channel would likely result in a lower signal to noise, but the system would be more applicable to laboratories globally. This is up to the discretion of scientists if they choose to use the sensor system, however, the system should be performed using both methods to compare the spectral characteristics of the systems.

Further discussion will assume the custom dye calibration method has optimized the quantization parameters for (**ss-PPi-mCPF**). The concentration of the sensor system should be optimized to be at the lowest level possible to still achieve effective quantification of DNA amplification through the entire replication process of qPCR. The fluorescence response in the sensor system is governed by the equilibrium with PPi and not through chelation and removal of PPi from solution: therefore, a minimal

concentration of the sensor system should be included to quantify the full dynamic range of [PPi] yet minimize the background fluorescence of the non-complexed sensor system. The concentration of sensor scaffold would also need to be optimized to assure that an excess of $[\text{Zn}(\text{NO}_3)_2]$ exceeding the range determined to not impede DNA replication is maintained and detrimentally impact the quality of the genomic data obtained.

Finally, the qPCR thermocycle procedures need to be optimized to effectively quantify DNA replication. The quantification of PPi by the sensor system is best obtained at (25 °C) where the binding constant between PPi and the sensor scaffold is greatest. An additional step in each cycle of the PCR reaction would be included in the thermocycle programming in which the temperature of the solution is decreased to 25 °C, allowed to reach equilibrium, and the fluorescence measurement taken before the next denaturation step of the next PCR cycle. This additional step should be optimized to the shortest time possible to minimize the background activity of Taq polymerase which may impede genomic analysis.

With optimized qPCR conditions, the experiment should be performed on several genes to determine the effects of amplicon sizes on DNA quantification efficiencies. Likewise, the results would need to be compared to SYBR Green and TaqMan probe methods to determine the relevant reaction efficiencies. The analysis would consist of cross comparisons between the systems' efficiency to reach a C_T for the target gene, dynamic range of quantification, and estimated cost of production to determine the impact of the novel sensing methodology for genomic studies.

With a completed system comes the opportunity to provide a cheaper alternative to current gold standard TaqMan probe methods of DNA quantification in qPCR. While the synthesis requires more expensive methods of purification, further industrial optimizations could be developed to achieve the most cost-effective method of product preparation. The system would be of great benefit to labs globally that may not have the funds nor resources available to develop and use TaqMan systems. Our system would provide an increased signal to noise over conventional SYBR Green methods: intercalator dyes often result in false positives due to coordination with initial DNA within the template samples.^{2,18} By bridging the gap between intercalator based and TaqMan probe based methods of real time DNA quantification, our PPi molecular sensor approach provides much opportunity to improve the sensitivity of a multitude of genomic applications to laboratories globally.

From my time working with Dr. Anzenbacher, and Dr. Halo, I have learned much of the world of synthetic chemistry and genomic studies, but I have also learned much about myself as a researcher and as an individual. For the past three years, I have worked under Dr. Anzenbacher in his research laboratory for which I have been able to

learn a multitude of applicable skills in organic chemistry synthesis. His expertise has allowed me to bridge a gap in education between lecture, laboratory, and into my career beyond. Most importantly, my time has allowed me to begin to think like a chemist rather than a chemistry student. These applicable skills will transfer beyond my current education and into my future as I pursue my next stages in life. Working with Dr. Halo has allowed for myself to bridge the gap between my focus in chemistry, and my minor in biology: I have been able to apply my research knowledge in chemistry in the multidisciplinary study of genomics and work towards a completely novel technique for qPCR sciences. Beyond multidisciplinary work, the experience to work within a genomic laboratory has allowed myself to increase my breadth of knowledge in genomic instrumentation and application that I had not experienced within my education at Bowling Green State University.

Most importantly, I have begun to learn to pace myself and understand my abilities within the world of scientific research and in time management as a student and researcher: over the past two years of the COVID-19 pandemic, I jumped into my schooling and research when life switched to being virtual. I have only now come to realize that I was stretching myself too thin between managing research, education, and life. It had been detrimental to my abilities and the stress of how I handled everything was far too overwhelming for anyone to manage. I realized that I had to step back from the next stages of this project's research to focus on myself as an individual and to complete my studies. From doing so, I am only now beginning to understand how to better manage my time, my studies, and to find my true self again so that I can best prepare myself for my future endeavors. In completing this honors project, I believe myself to be successful in the goals set by its creation. I have gained important first-hand knowledge into the multidisciplinary work of applied chemical synthesis as it pertains to the development of a novel sensor for genomic studies, have worked to develop the critical thinking skills required to develop the project and execute the project, and have developed the skills in writing and project presentation to produce this work. With these points being made, I have best prepared myself to complete this project and prepare for my future set before me.

Experimental:

Synthesis of DPA precursor:

Three reactions were performed to synthesize DPA, (*N,N*-bis(2-pyridylmethyl)ethylenediamine) (**4**) from modified procedures.¹⁹ Commercially available ethylenediamine (**1**) was reacted with di-*tert*-butyldicarbonate (Boc₂O) to produce (**2**) which was reacted with commercially available picolyl chloride to produce (**3**). Finally, deprotection of the Boc group was performed using trifluoroacetic acid (TFA) to form the final DPA precursor (**4**) (Figure E1).

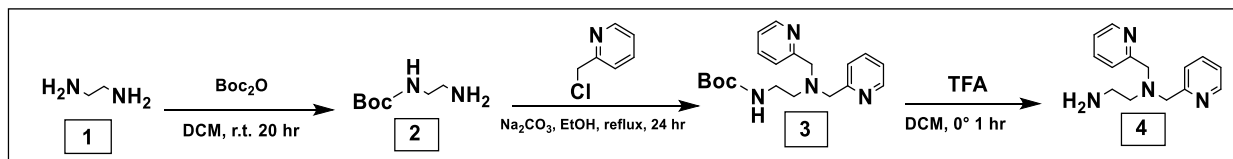


Figure E1: Synthetic scheme for the preparation of DPA precursor (**4**) from commercially available reagents.

Tert-butyl (2-aminoethyl)carbamate (**2**):

To a solution of ethylenediamine (23.70 ml, 353.75 mmol) in 265 ml DCM cooled to 0°C, was added di-*tert*-butyl dicarbonate (8.2 ml, 35.375 mmol) in 177 ml DCM dropwise over 6 hours. The resulting mixture warmed to room temperature, was stirred for 14 hours, and evaporated to dryness. The solution was dissolved in saturated NaHCO₃, extracted three times with DCM, washed with brine, dried over anhydrous Na₂SO₄, filtered, and evaporated to dryness to afford (**2**) (4.995 g, 86.5%) as a colorless oil.

N-tert-butoxycarbonyl-N',N'-bis(2-pyridylmethyl)ethylenediamine (**3**):

To a solution of **2** (4.9853 g, 31.12 mmol) in 200 ml EtOH was added anhydrous Na₂CO₃ (14.545 g, 137.6 mmol) and 2-(chloromethyl)pyridine hydrochloride (11.232 g, 68.47 mmol). The mixture was refluxed under N₂ for (21 hr.). The reaction mixture was evaporated to dryness and suspended in 200 ml 2M NaOH, extracted with DCM (70 ml x3), washed with brine (40ml), dried over Na₂SO₄, filtered, and evaporated to dryness. Half of the crude sample was purified by aluminum oxide Vacuum Flash Column Chromatography (EtOAc 100%) to afford **2c** (3.507 g).

N,N-Bis(2-pyridylmethyl)ethylenediamine (**4**):

To a solution of **2c** (3.4938 g, 10.23 mmol) in 7 ml DCM cooled to 0°C was added dropwise, 8 ml of TFA. The flask was fitted with a condenser and septum then warmed to room temperature. Reaction progression was monitored by TLC (Al₂O₃, 95:5, EtOAc:MeOH). After 6hr, the volatiles were evaporated. The crude was dissolved in 2M

NaOH until basic and extracted three times with DCM, washed with brine, and evaporated to dryness to afford **2d** (2.373 g, 96% yield) as a free-flowing orange oil.

Optimization screening reactions for the synthesis of N-3-Dihydroxyborylbenzyl-N',N'-bis(2-pyridylmethyl)ethylenediamine molecular sensor scaffold:

Synthesis of the sensor scaffold compound was performed using modified reductive amination procedures by Nonaka et al (Figure **E2**).¹⁰

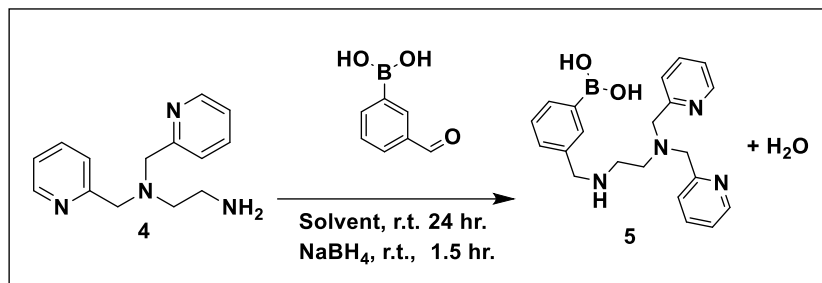


Figure E2: Synthesis of molecular sensor scaffold by reductive amination procedures.

N-3-Dihydroxyborylbenzyl-N',N'-bis(2pyridylmethylethyl)enediamine:

For the screening reactions three different solvents were tested: EtOH, MeOH, and DCE. To the reactions carried out in MeOH and DCE, two reactions were performed: one with the addition of 1 drop glacial AcOH and one without (see Table **E1** for mass). stir bar, and approximately 30 mg 3Å molecular sieves was loaded into a dried 5ml flask equipped with Claisen adapter, gas line adapter and septum. To a second 5 ml flask was loaded 3-formylphenylboronic acid (see Table **E1**, stir bar, and 30 mg 3Å molecular sieves. Equipped with the Claisen adapter, gas adapter, and septum, both flasks were purged with N₂. The solvents (1.25 ml) that had been dried over 25% m/v 3Å molecular sieves overnight was added with a dried needle to **4**. The resulting solution was transferred to the second flask using 0.7 ml of solvent to rinse. To the reactions utilizing catalytic acid, one drop AcOH was added through the septum. The resulting solution was stirred overnight under N₂. NaBH₄ (see Table **E1** was added under N₂ and left to stir for 2 hr. Reaction mixture was evaporated to dryness and 1 mg of crude material was suspended in 95:5 H₂O:MeOH with 0.1% TFA at 1 mg/ml concentration. Filtered through a 0.2 μm filter, 100 μL of crude solution was analyzed by RP HPLC to afford *t_r* and relative % composition for the target peaks.

Table E1: Screening reactions: masses of reagents used.

| Reaction Conditions | DPA-en ligand mass | 3-formylphenylboronic acid mass | NaBH ₄ mass |
|---------------------|--------------------|---------------------------------|------------------------|
| EtOH w/o AcOH | 30.2 mg | 18.6 mg | 9.6 mg |
| MeOH w AcOH | 31.1 mg | 19.2 mg | 10.3 mg |
| MeOH w/o AcOH | 29.8 mg | 18.8 mg | 9.4 mg |
| DCE w AcOH | 30.6 mg | 18.6 mg | 9.6 mg |
| DCE w/o AcOH | 30.7 mg | 18.7 mg | 9.6 mg |

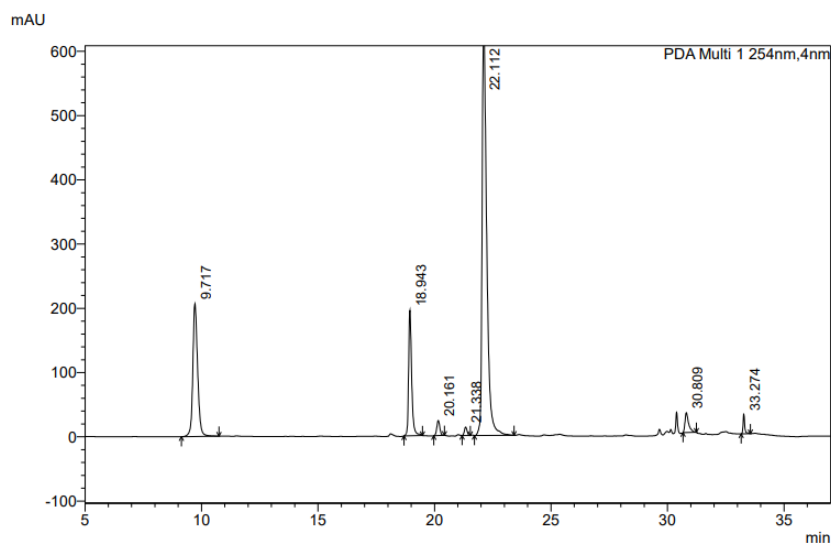


Figure E3: HPLC chromatogram of sensor scaffold synthesis in DCE w/o AcOH: HPLC gradient of 95:5 H₂O with 0.1% TFA: MeOH. Product peak, $t_R = 22.112$.

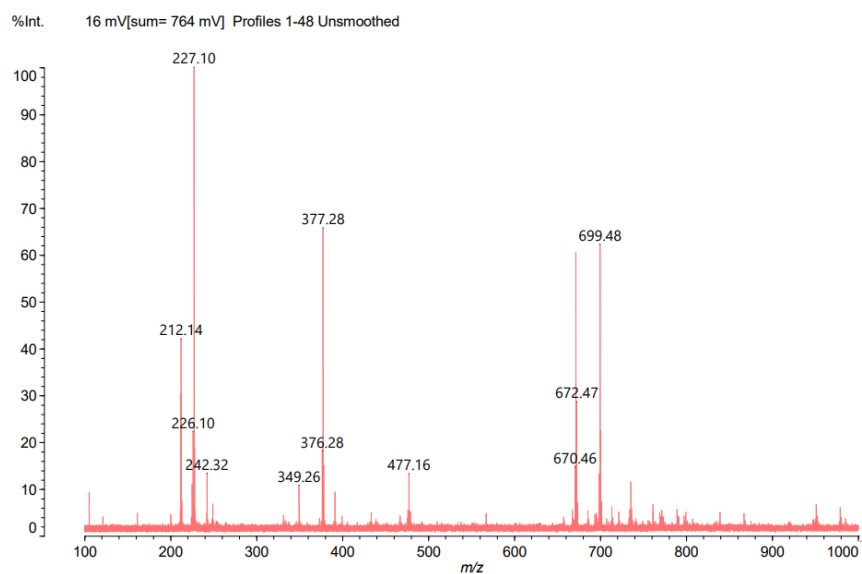


Figure E4: MALDI mass spectrum of the product peak, reaction ran in EtOH:

$M+1 = 377.28$ m/z.

First scaled-up synthesis of *N*-3-Dihydroxyborylbenzyl-*N',N'*-bis(2pyridylmethylethyl)enediamine molecular sensor scaffold:

Similar procedures as to the screening reactions were performed for the scaled-up synthesis. To a 25ml flask was charged 61.88 mg of 3-formylphenylboronic acid (3-FPBA) and ~ 37 mg of 4 Å molecular sieves and a stir bar. To a second 10 ml flask was charged (**4**) 100 mg. Both flasks were fitted with Claisen adapters and purged with N₂. DCE (5 ml) was added to the flask containing (**4**) and the resulting solution was transferred to the flask containing (3-FPBA) using DCE (1.5 ml) to rinse. The resulting solution was left to react under N₂ overnight and 31.3 mg of pelletized NaBH₄ was added and left to react for two hours. The crude was then dried and purified by RP-ACC (SNAP C18 30g). Gradient elution (initial conditions, in 95:5 H₂O:MeOH with 0.1% TFA) were used for purification. Two purifications were performed as the crude was not soluble in the 95:5 H₂O:MeOH with 0.1% TFA used for wet loading of the column: the second purification used the crude that was dissolved into minimal MeOH (100%). ¹H NMR showed a lack of product formation for both purification steps.

Second scaled-up synthesis and purification of *N*-3-Dihydroxyborylbenzyl-*N',N'*-bis(2pyridylmethylethyl)enediamine molecular sensor scaffold:

The second scale up used a procedure modified from the first scale up reaction to improve the reductive amination reaction. To an oven dried 150 ml flask was charged 3-FPBA (473.0 mg), and 4 Å molecular sieves (485 mg). To a second 100 ml flask was charged **4** (842.6 mg). Both flasks were fitted with a Claisen adapter and purged with N₂ through both septums. To **4** was added 49 ml of dried MeOH and the resulting solution was transferred to the flask containing the 3-FPBA and rinsed with MeOH (6 ml). The resulting solution was left to stir overnight under N₂ and mortar ground NaBH₄ (500.0 mg 4 mol eq.) was added. The solution was left to react for two hours. The mixture was filtered through a frit and dried to completion.

Two purifications by RP-ACC were required to pre-purify the compound. 894.8 mg of crude were dissolved into minimal 95:5 H₂O:MeOH with 0.1% TFA and purified by RP-ACC (SNAP C18 60g, gradient elution with initial conditions of 95:5 H₂O:MeOH with 0.1% TFA). Fractions 10-20 resulted in 451 mg of purified material. Overloading of the column and ¹H NMR analysis showed that the compound was impure. The second purification of crude (451 mg) by RP-ACC (SNAP C18 60g, gradient elution with initial conditions of 95:5 H₂O:MeOH with 0.1% TFA) was performed. Fractions 17-35 were collected and dried to yield 204.5 mg of pre-purified compound: ¹H NMR analysis showed a higher purity, yet impure product.

RP-HPLC was performed to finalize the purification of the sensor scaffold compound. 102.66 mg of pre-purified scaffold compound was dissolved into 900 μL of 95:5 H_2O :MeOH with 0.1% TFA, and filtered through a 0.2 μL filter. 100 μL sample injections were used within the semi-prep RP-HPLC. An optimized gradient elution (25 min, 95-60% H_2O in MeOH with 0.1% TFA) was used for all purifications. The purified sensor scaffold was obtained in a 33.96 mg yield. ^1H NMR and ESI-MS confirmed the formation and purity of the product formed.

Freebase extraction of *N*-3-Dihydroxyborylbenzyl-*N',N'*-bis(2pyridylmethylethyl)enediamine molecular sensor scaffold:

The HPLC purified product (27.38 mg) was dissolved into minimal saturated Na_2CO_3 until bubbling stopped and was rinsed into a small separatory funnel using DCM. The solution was extracted with DCM (4x), dried with Na_2SO_4 (anhy.), filtered, dried, and dried on the high vacuum line for 24 hr. The product was obtained, 11.00 mg (40.18% yield) as an opaque white oil. Further NMR and MALDI analysis was unable to be performed due to time constraints.

Coordination of the molecular sensor scaffold to $\text{Zn}(\text{NO}_3)_2$:

Procedures were followed according to the conditions reported by Nonaka et al.¹⁰ To a 25 ml round bottom flask was charged 100.28 mg of RP-ACC pre-purified compound dissolved into 9 ml of MeOH. $\text{Zn}(\text{NO}_3)_2 \times 6\text{H}_2\text{O}$ (79.055 mg, 1 mol eq) was charged to the round bottom and allowed to stir at room temperature for 1hr. the resulting crude solution was evaporated and a recrystallization from dry THF was performed. From this reaction 13.8 mg of impure active sensor scaffold compound was produced: ^1H NMR showed the presence of multiple impurities and a mixture of coordinated and uncoordinated product.

Determination of the effect of $\text{Zn}(\text{NO}_3)_2$ on the qPCR reaction:

The qPCR reaction was performed with a series of increasing $\text{Zn}(\text{NO}_3)_2$ concentrations to determine the system's tolerance to excess Zn^{2+} ions in solution. A $\Delta\Delta\text{C}_q$ qPCR experiment was performed in which the expression of GapDH gene was compared to the reference Env gene in genomic CDNA from dog samples. The following concentrations of $\text{Zn}(\text{NO}_3)_2$ were prepared from 20 μM stock solution dissolved into DNAase free and RNAase free MilliQ water: 0.0, 0.5, 1.0, 2.0, 3.0, 4.0, 5.0 μM final concentrations (20 μL qPCR reactions) (48 well qPCR plate). Triplicate measurements of each gene were made for each reaction. Reactions were prepared for the following volume of reagent per reaction: 10 μL Power SYBR™ Green PCR Master Mix, 0.2 μL forward DNA primer. 0.2 μL reverse DNA primer, 3.6 μL DNAase free and RNAase free MilliQ water, 0.0-5.0 μL of 20 μM $\text{Zn}(\text{NO}_3)_2$ stock solution, and 5.0-0.0 μL DNAase free and RNAase free MilliQ water (volume of the two final reagents equals 5.0

μL). Two master mixes were created in which the forward and reverse primers related to the GapDH or Env gene amplified. The well plate was prepared and loaded into the qPCR machine under standard SYBR green conditions (with modified initial denaturing, and annealing times) and allowed to run to completion. Average C_T values were determined from working reactions of each triplicate set.

References:

- (1) Gharizadeh, B.; Nordström, T.; Ahmadian, A.; Ronaghi, M.; Nyrén, P. Long-Read Pyrosequencing Using Pure 2'-Deoxyadenosine-5'-O'-(1-Thiotriphosphate) Sp-Isomer. *Anal. Biochem.* **2002**, *301* (1), 82–90.
<https://doi.org/10.1006/abio.2001.5494>.
- (2) Singh, J.; , Niti Birbian, S. S. and A. G. A Critical Review on PCR, Its Types and Applications. *Int. J. Adv. Res. Biol. Sci.* **2014**, *1* (7), 65–80.
- (3) Abhishek, A.; Doherty, M. Update on Calcium Pyrophosphate Deposition. *Clin. Exp. Rheumatol.* **2016**, *34* (4), 32–38.
- (4) Wilson, M. S. C.; Livermore, T. M.; Saiardi, A. Inositol Pyrophosphates: Between Signalling and Metabolism. *Biochem. J.* **2013**, *452* (3), 369–379.
<https://doi.org/10.1042/BJ20130118>.
- (5) VanGuilder, H. D.; Vrana, K. E.; Freeman, W. M. Twenty-Five Years of Quantitative PCR for Gene Expression Analysis. *Biotechniques* **2008**, *44* (5), 619–626.
<https://doi.org/10.2144/000112776>.
- (6) Bustin, S. A. *A-Z of Quantitative PCR*; International University Line, 2004.
- (7) Xu, Z.; Ren, Y. Y.; Fan, X.; Cheng, S.; Xu, Q.; Xu, L. A Naphthalimide-Based Fluorescent Probe for Highly Selective Detection of Pyrophosphate in Aqueous Solution and Living Cells. *Tetrahedron* **2015**, *71* (31), 5055–5058.
<https://doi.org/10.1016/j.tet.2015.05.111>.
- (8) Cho, H. K.; Lee, D. H.; Hong, J. I. A Fluorescent Pyrophosphate Sensor via Excimer Formation in Water. *Chem. Commun.* **2005**, No. 13, 1690–1692.
<https://doi.org/10.1039/b417845a>.
- (9) McDonough, M. J.; Reynolds, A. J.; Lee, W. Y. G.; Jolliffe, K. A. Selective Recognition of Pyrophosphate in Water Using a Backbone Modified Cyclic Peptide Receptor. *Chem. Commun.* **2006**, No. 28, 2971–2973.
<https://doi.org/10.1039/b606917g>.
- (10) Nonaka, A.; Horie, S.; James, T. D.; Kubo, Y. Pyrophosphate-Induced Reorganization of a Reporter-Receptor Assembly via Boronate Esterification; A New Strategy for the Turn-on Fluorescent Detection of Multi-Phosphates in Aqueous Solution. *Org. Biomol. Chem.* **2008**, *6* (19), 3621–3625.
<https://doi.org/10.1039/b808027e>.
- (11) Lee, J. H.; Jeong, A. R.; Jung, J. H.; Park, C. M.; Hong, J. I. A Highly Selective and Sensitive Fluorescence Sensing System for Distinction between Diphosphate and Nucleoside Triphosphates. *J. Org. Chem.* **2011**, *76* (2), 417–423.
<https://doi.org/10.1021/jo1017102>.
- (12) Bartlett, J. M. S.; Stirling, D. *A Short History of the Polymerase Chain Reaction*, 2ns ed.; Humana Press: Totowa, 2003.

- (13) Lee, L. S.; Till, B. J.; Hill, H.; Huynh, O. A.; Jankowicz-Cieslak, J. *Mutation and Mutation Screening BT - Cereal Genomics: Methods and Protocols*; 2014.
- (14) Heid, C. A.; Stevens, J.; Livak, K. J.; Williams, P. M. Real Time Quantitative PCR. *Genome Res.* **1996**, *6*, 986–994. <https://doi.org/10.1016/b978-012372185-3/50024-9>.
- (15) Tajadini, M.; Panjehpour, M.; Javanmard, S. Comparison of SYBR Green and TaqMan Methods in Quantitative Real-Time Polymerase Chain Reaction Analysis of Four Adenosine Receptor Subtypes. *Adv. Biomed. Res.* **2014**, *3* (1), 85. <https://doi.org/10.4103/2277-9175.127998>.
- (16) Jothikumar, P.; Hill, V.; Narayanan, J. Design of FRET-TaqMan Probes for Multiplex Real-Time PCR Using an Internal Positive Control. *Biotechniques* **2009**, *46* (46), 519–524.
- (17) Systems, S. R. P. C. R. Custom Dye Calibration for StepOne™ And.
- (18) Mackay, I. M. Real-Time PCR in the Microbiology Laboratory. *Clin. Microbiol. Infect.* **2004**, *10* (3), 190–212. <https://doi.org/10.1111/j.1198-743X.2004.00722.x>.
- (19) Hanaoka, K.; Kikuchi, K.; Urano, Y.; Nagano, T. Selective Sensing of Zinc Ions with a Novel Magnetic Resonance Imaging Contrast Agent. *J. Chem. Soc. Perkin Trans. 2* **2001**, *1* (9), 1840–1843. <https://doi.org/10.1039/b100994j>.